Application of the PC-SAFT Equation of State to Asphaltene Phase Behavior

P. David Ting,[1,2] Doris L. Gonzalez,[2] George J. Hirasaki,[2] and Walter G. Chapman[2]

1 – Work performed while at RiceUniversity, Currently with Shell Global Solutions (US) Inc., Westhollow Technology Center, Houston, TX 77082

2 - Department of Chemical Engineering, Rice University, Houston, TX 77005

Abstract

A method to characterize crude oil including asphaltenes using the perturbed chain form of the statistical associating fluid theory (PC-SAFT) is presented. The theory accurately predicts the bubble point, density, and asphaltene precipitation onset for the oil. Examples show that the theory predicts asphaltene instability due to changes in pressure, temperature, and fluid composition. Further work demonstrates the effect of asphaltene polydispersity and resins on the phase behavior of asphaltenes. The approach demonstrates that laboratory and field observations of asphaltene phase behavior can be explained based only on molecular size and van der Waals interactions.

I. Introduction

This chapter provides an application of the Statistical Associating Fluid Theory (SAFT)[1-4] equation of state (EOS) to model the effects of pressure, temperature, and composition on the phase behavior and stability of asphaltenes in crude oil. SAFT is a versatile molecular model capable of predicting the effects of molecular shape, van der Waals forces, polar interactions, and association on the thermodynamic properties and phase behavior of fluids. The approach we

have taken is to use the minimum number of (physically relevant) parameters possible to describe phase behavior of asphaltenes by including only essential interactions.

Given the high degree of complexity of crude oil and its large variability in composition due, in part, to differing source rock properties and migration history, one may question the relevance of a molecular based model in light of our current understanding of asphaltenes. It is our belief that the bulk phase behavior of asphaltenes can be accurately described if we can correctly account for its major physical attributes and its interactions with other species in oil. There are many advantages in using a predictive molecular based EOS model. For instance, the sensitivity of asphaltene phase behavior to the effects of temperature, pressure, and asphaltene polydispersity can be quickly and confidently modeled. An EOS framework can also be more readily implemented into existing reservoir and thermal-hydraulic simulators used in industry. At the other end of the scale, the EOS approach, when compared to more rigorous molecular simulations, has the advantage of speed and ease of use. This comes, of course, at the expense of detailed descriptions at the molecular level.

With the molecular basis of the SAFT approach, it is necessary to define the system to be modeled. Our viewpoint is described and justified in the Section I of this chapter. In Section II, we present in detail the characterization of an oil with SAFT including applications to asphaltene phase behavior on reservoir depressurization and gas injection. Conclusions are provided in the final section.

I.A. Asphaltene Properties & Field Observations

The currently accepted definition of asphaltenes is an operational one based on solubility (i.e., asphaltenes are insoluble in heptane or pentane and soluble in toluene). As such, it reveals little about the structure of asphaltenes. Most researchers agree that asphaltenes are a polydisperse mixture of molecules containing polynuclear aromatic, aliphatic, and alicyclic moieties with small amounts of dispersed heteroelements such as oxygen, sulfur, nitrogen, vanadium, and nickel. When compared to other crude oil components, asphaltenes are the heaviest fraction of a distribution (in molecular weight as well as aromaticity) of compounds that include aromatics and resins in the lower molecular weight sub-fractions. The accepted definition for asphaltenes is, in essence, an arbitrarily divided sub-fraction of this distribution. Asphaltenes are more aromatic (low H/C ratio) than most other oil fractions, are larger in molecular weight, and have higher solubility parameter.[5]

The interesting phase behavior of asphaltenes in oil can be deduced by studying a few representative examples of field experiences with asphaltene problems.[6-11] These examples not only elucidate asphaltene behavior typically seen in the field and in PVT laboratories but also help us gain a better understanding of the type of molecular interactions between asphaltenes and other oil species. From these experiences, it can be concluded that asphaltenes are usually stable in heavier oils well above the bubble point pressure under reservoir conditions. Light oils with little asphaltenes are the most susceptible to asphaltene problems. Field operators have reported that asphaltenes are unstable over a range of pressures during reservoir depressurization. More specifically, the effect of pressure on asphaltene phase separation is most pronounced for light oil near the bubble point. Asphaltenes are stable at high pressure and at pressures well below the

bubble point, but, in many cases, they are unstable at pressures somewhat above and below the bubble point. Far below the bubble point, asphaltenes tend to be stable since most of the precipitants (methane, ethane, nitrogen, etc.) have escaped from the liquid. Compositional changes such as oil blending or miscible flooding sometimes result in asphaltene precipitation. Interestingly, temperature changes may result in either asphaltene precipitation or solubilization. For instance, in the propane deasphalting process, asphaltenes become increasingly unstable with temperature increase.[12] However, for n-alkane (n-C_{5+}) titrations, asphaltene stability improves with increasing temperature.[12] These examples highlight the need, by such disciplines as flow assurance and production engineers, for a predictive model that is capable of explaining these observations.

A distinction needs to be made between thermodynamic asphaltene stability (which is the focus of this work) and asphaltene-related field problems. Just because asphaltenes may become unstable during production does not necessarily mean that deposition will be encountered. Factors such as (1) the properties of the asphaltene that precipitated including its "stickiness", (2) the amount of the asphaltene that precipitated, and (3) the flow pattern in the production system (flowline, tree, riser, inside topside facility, etc.) all play a role in determining whether the precipitated asphaltenes will result in field problems. However, the ability to accurately model asphaltene as a polydisperse system will help in elucidating its deposition tendencies. Finally, it is important to note that asphaltene from one region (source) may have very different properties than asphaltene from another region.

I.B. The Two Views of Asphaltene Interactions

In the last 50+ years, two views to describe the phase behavior of asphaltenes have emerged. In one view, which we will call the "molecular solution" approach, asphaltenes are treated as molecules that are solubilized by the oil. Asphaltene precipitation is treated as liquid-liquid or solid-liquid equilibria. The hypothesis in this framework has been that molecular size and van der Waals interactions, which are related to molecular polarizability, dominate asphaltene phase behavior in reservoir fluids; the more polarizable components (the resins and aromatics) solubilize the asphaltenes and the less polarizable components (saturates) destabilize the asphaltenes. Proponents of this view have used such approaches as Flory-Huggins theory[13] or equations of state to model asphaltene phase behavior.[14-18] In this chapter we report on the application of the SAFT equation of state to model asphaltene phase behavior.[19,20] Although the SAFT approach and its extensions can account for polar and association effects, we find that the effects of molecular size and van der Waals attractions are sufficient to explain reported observations of asphaltene phase behavior.

The application of Flory-Huggins-regular solution theory to describe asphaltene phase behavior was first proposed by Hirschberg, *et al.*[15] While the Flory-Huggins-regular solution based approaches have been used with varying success to model asphaltene solubility with n-alkane titrations under ambient conditions, it is difficult to extend the approach to model asphaltene solubility under reservoir conditions. In a sense, the theory is not a "complete" equation of state; it requires the molar volumes and solubility parameters under reservoir conditions. These values must be obtained from an equation of state or estimated from empirical correlations. For example, in the work of Chung, *et al.*,[21] the Flory-Huggins-regular-solution model is combined

with the Peng-Robinson cubic equation to model asphaltene solubility in oil. And in the work of Burke, *et al.*,[22] the Flory-Huggins-regular-solution model parameters were obtained from the Zudkevitch-Joffe-Redlich-Kwong equations. Some success in predicting asphaltene precipitation at reservoir conditions from Flory-Huggins parameters fit to ambient titration data has been reported using an extrapolation due to Wang and Buckley.[14, 23]

Another limitation of the Flory-Huggins model is its inability to predict certain classes of phase behavior. As an example, the model requires temperature dependent binary interaction parameters to show lower critical solution behavior, phase behavior known to occur in systems with large size differences between molecules.

Another popular classical thermodynamics approach to model asphaltene behavior is to use cubic equations of state. In the method proposed by Nghiem, *et al.*,[24] the C_{31+} heavy end of crude oil is first divided into nonprecipitating and precipitating sub-fractions. Different interaction parameters (between these sub-fractions and light ends) are then assigned to reproduce experimental results. In another example, Akbarzadeh, *et al.*[16] modified the Soave-Redlich-Kwong cubic equation by adding an additional aggregation size parameter to asphaltenes. The cubic equations have relatively simple functional forms and are easy to implement into existing reservoir simulators because cubic equations have been used extensively to describe the thermodynamic behavior of reservoir fluids. However, the major shortcoming of cubic equations of state is that they cannot describe the phase behavior of systems with large size disparities[25] and that they cannot accurately describe liquid densities. Accurate modeling of liquid density is essential for an equation of state to predict liquid-liquid equilibria over a range of conditions.

While the calculated densities can be modified using volume translation techniques, volume translations do not affect phase equilibria calculations.

In our approach, asphaltene instability is modeled as liquid-liquid equilibria. We have chosen to base our model on the SAFT equation of state because of its ability to accurately model fluid densities as well as phase behavior for mixtures with substantial size asymmetry.[20, 25] SAFT and its extensions also explicitly account for association and polar interactions. The details of the model are discussed in section II.

As noted above, the "molecular solution" approach is not the only approach used in literature to describe asphaltene phase behavior in oil. In this other approach generically called the "micellar" approach, the structural characteristics of asphaltenes and resins are emphasized - asphaltenes are viewed to be stabilized by resins via polar-polar interactions. The basis of this viewpoint is that asphaltenes and resins are the most polar fractions of crude oil because they contain heteroatoms of various proportions. When resins are added, less asphaltenes will precipitate. And when n-alkanes are added, asphaltenes will precipitate because of the dilution of resins in the mixture. The argument is that resins stabilize asphaltenes in a similar way to surfactants stabilizing a micro-emulsion in an oil/water mixture. Thermodynamic models that take the micellar view include the solid-asphaltene colloidal model proposed by Leontaritis and Mansoori,[26] the reversible micellization model proposed by Victorov and Firoozabadi,[27] and the McMillan-Mayer-SAFT based theory proposed by Wu.[12, 28, 29] Interestingly, the SAFT framework is versatile enough that it has been used to develop models for both points of view.

I.C. Our View and Approach

The underlying hypothesis of our approach in modeling asphaltene phase behavior is that molecular size and nonpolar van der Waals interactions dominate asphaltene phase behavior in reservoir fluids. We find that the phase behavior described in field and laboratory experiences are similar to those seen in oligomer and polymer systems. For instance, the pressure, temperature, and compositional behavior of asphaltenes in reservoir fluid described in Section 1.1 is qualitatively similar to the behavior of polystyrene in a mixture of cyclohexane and CO_2.[30] In such systems, the phase behavior can be predictively modeled by only considering molecular size and van der Waals interactions. Note that the existence of other types of intermolecular interactions are not being discounted or trivialized in our framework; we are simply taking the approach that the behavior of asphaltenes in crude oil systems can be described to a large extent by accounting for molecular size and van der Waals interactions only.

Our hypothesis is supported by other evidence. For instance, an investigation of asphaltene solubility in over 40 polar and nonpolar solvents by Wiehe[31] shows that asphaltenes are soluble in solvents with high field force solubility parameters (which is a measure of nonpolar, van der Waals interaction strength) and insoluble in solvents with moderate and high complexing solubility parameters (which is a measure of hydrogen bonding and polar interaction strengths). While this observation is consistent with the idea that van der Waals interactions determine asphaltene phase behavior, it does not readily fit in the micellar framework.

As another example, consider that some relatively nonpolar molecules of similar size and structure can be either precipitants or solvents for asphaltenes. Toluene ($C_6H_5CH_3$) is a good

solvent for asphaltenes while n-heptane (C_7H_{16}) is a precipitant. Similarly, both carbon disulfide (CS_2) and carbon dioxide (CO_2) are weakly polar and of similar molecular structure, but CS_2 is a good solvent for asphaltenes while CO_2 is a precipitant. In these examples, the more polarizable molecules (such as toluene and carbon disulfide, molecules with the stronger van der Waals interactions as shown by their solubility parameters) are the better solvents for asphaltenes.

In some situations, the role of polar or hydrogen bonding interactions is important. For example, asphaltenes may aggregate on the water-oil interface and stabilize water emulsions.[32] Also, addition of a sufficiently large amount of alkyl-benzene derived amphiphiles (such as dodecyl benzene sulfonic acid) can inhibit asphaltene aggregation.[33] While polar interactions may play a role, our hypothesis is that asphaltene phase behavior in the reservoir, such as on reservoir depressurization, is shaped to a larger extent by the nonpolar interactions in the oil.

Recent structural investigations on asphaltene behavior[34] suggest that multiple levels of interactions may be occurring in fluids containing asphaltenes. In all except very good solvents and under near-infinite dilution concentrations, asphaltenes exist as molecular aggregates (of several units, each ~500-800 amu in size) and each aggregate behaves as if it is a single molecule. Our approach at this point is to assume that asphaltenes have pre-aggregated in crude oil systems and that the asphaltenes in our model would, in fact, exhibit characteristics of the molecular aggregate so that the molecular weight in our model represents the MW of the aggregate. This approach is justified since oil systems (and the model systems investigated in this work) are neither infinitely dilute in asphaltenes nor very good solvents for asphaltenes.

II. Introduction to SAFT

We adopt the SAFT equation of state for our study of asphaltenes because of its demonstrated ability to accurately describe and predict the effects of large molecular size differences and association on phase behavior of complex mixtures.[25, 30, 35, 36] This has been seen in numerous applications of SAFT to polymer solutions and hydrogen bonding fluids. For example, SAFT has become an important tool in predicting polymer phase behavior to prevent fouling in polymer processing.[37]

SAFT was developed by Chapman, et al.[1, 2, 3] based on extensions and simplifications of Wertheim's theory for associating fluids.[38, 39, 40, 41] In SAFT, molecules are modeled as chains of bonded spherical segments. As shown in Figure 1, SAFT determines the free energy of a fluid as the sum of the free energy for a collection of spherical "segments" (from which molecules are constructed) plus the change in free energy on "bonding" these spherical "segments" in a prescribed manner to form the molecules of interest. This change in free energy can be calculated from Wertheim's theory. Finally, if the molecules have association sites, the change in free energy due to these directional interactions are explicitly accounted for using Wertheim's theory.

A theory like SAFT that is based in statistical mechanics offers several advantages. The first advantage is that each of the approximations made in the development of SAFT such as the chain and association terms has been verified against molecular simulation results.[1] In this way, the range of applicability and the shortcomings of each term in the equation of state have been assessed. A second advantage is that the SAFT parameters have physical meaning. For

example, a chain molecule is characterized by the diameter or volume of a segment, the number of segments in the chain, and the segment-segment van der Waals attraction. These parameters are, in general, fit to saturated liquid densities and vapor pressures for the pure components. Since the equation of state parameters are physical, they behave systematically within a homologous series. Furthermore, parameters for new systems can be estimated from those of previously modeled systems. In this way, parameters for saturates, aromatics, and resins can quickly be determined to model a crude oil.

Numerous forms of the SAFT equation of state have been proposed.[1-4, 42-44] These forms differ only in the segment term used to account for the van der Waals attraction between molecules; all use the same chain and association terms as introduced in the original SAFT papers by Chapman, et al.[1-3, 42] Because each of these SAFT versions shares the same basic form of the equation of state, they each give similar results. In this work, we report results using the Perturbed Chain version of SAFT or PC-SAFT due to Gross and Sadowski.[4] We expect qualitatively similar results if another version of SAFT is used instead.

II.A PC-SAFT Pure Component Parameters

For each non-associating species in SAFT, the equation of state requires the specification of three physical parameters: σ, the diameter of each molecular segment, m, the number of segments in the molecule, and ε/k, the interaction energy (van der Waals attraction) between each molecular segment. A list of PC-SAFT parameters for compounds of interest to this work is given in Table 1.

An important feature of SAFT is that the fitted pure component parameters (σ, m, and ε/k) behave in a systematic manner with molecular weight for different classes of compounds[4, 45] (see Figure 2). Furthermore, species with both aromatic and aliphatic characteristics have EOS parameters that lie in between the aromatic and n-alkane correlations in a systematic manner depending on their degree of aromaticity or aliphaticity. For instance, the parameters for benzene derivatives and cyclo-alkanes approach the pure component parameters of the alkanes as the degree of aliphaticity increases. These "well-behaved" correlations between the pure component parameters and molecular weight have three implications. (1) SAFT parameters for crude oil components or lumps of components (pseudo-components) can be estimated from their average molecular weights. (2) SAFT parameters can be estimated for substances whose vapor pressures and/or liquid densities are difficult to measure. In the case of asphaltenes, the correlations of aliphatic and aromatic SAFT parameters with molecular weight provide the upper and lower bounds of the asphaltene SAFT parameters. And (3) the "well-behaved" pure component SAFT correlations imply that the EOS can easily be extended to model the effects of polydispersity.

Note that the systematic behavior shown in Figure 2 has been observed for a number of SAFT implementations (see previous section). Discussions from this point on will focus on the use of PC-SAFT.

II.B PC-SAFT Characterization of a Recombined oil

To use the SAFT equation of state to model live oil systems, we need to be able to account for the fluid's (PVT) phase behavior using a minimum number of real components and "realistic"

pseudo-components. In this section, we will outline (1) a method to model live oil systems using a small number of real components and pseudo-components and (2) a method to characterize asphaltenes in the SAFT model. Both (1) and (2) take advantage of the systematic SAFT parameter-molecular weight behavior discussed in Section II.A.

Consider the application of PC-SAFT to a recombined "live" oil (separator oil plus its associated gas) for which the bubble point, GOR, stock tank oil density (API gravity), density above saturation, and asphaltene precipitation onsets have been measured.[47] To model the phase behavior of the recombined oil, the oil is treated as a mixture of six pseudo-components (Figure 3). Three sub-fractions (methane, N_2+CO_2, and light n-alkanes) are used to describe the separator gas and three sub-fractions (saturates, aromatics+polynuclear aromatics, and asphaltenes) are used to describe the stock tank oil.

The relative amount of each sub-fraction given in Figure 3 can be calculated based on composition data from gas chromatography (GC), SARA fractionation data, and GOR data. The lumping of N_2 with CO_2 was appropriate in this case because very little CO_2 was present. More generally, we treat N_2 and CO_2 as separate components.

Note that the proposed lumping scheme introduces a small error in the description of the fluid properties. This is because there are non-negligible amounts of light n-alkanes such as butane and pentane partitioned in both the "light n-alkane" pseudo-components and the "saturates" pseudo-component. However, the effect of this error on the fluid phase behavior was found to be small.

II.B.1 Characterization of Separator Gas

The three PC-SAFT parameters (σ, m, and ε/k) for each pseudo-component are related to the average molecular weight of that pseudo-component. Parameters for the pseudo-components can be interpolated/extrapolated from correlations shown in Figure 2. For instance, the PC-SAFT parameters for the "light n-alkane" pseudo-component lie on the n-alkane correlations in Figure 2 with an average molecular weight of 47. For a real component, PC-SAFT parameters are taken from fits to the component's saturated liquid densities and vapor pressures. Parameters for the separator gas real- and pseudo-components are given in Table 2.

To accurately describe the van der Waals attraction between unlike pairs of molecules, the energies of interaction are often modified in an equation of state via the use of binary interaction parameters. The binary interaction parameters used in this work were fit to vapor-liquid equilibria data, with the values listed in Table 3.

The PC-SAFT calculated density of 0.3708 g/cm^3 obtained from the three pseudo-component treatment of the separator gas compares well with the measured density of 0.3773 g/cm^3 at 241.3 bar and 293K.

II.B.2 Characterization of Stock-Tank Oil

The stock-tank oil is treated as a mixture of 3 pseudo-components (saturates, aromatics+resins, and asphaltenes). This particular division was set up partly to take advantage of the SARA

fractionation data. Unlike SARA, which breaks down an oil into saturates, aromatics, resins, and asphaltenes, we grouped aromatics and resins into one single pseudo-component because they form a part of the same distribution in molecular weight and aromaticity (that actually extends out to the asphaltenes). The following assumptions are applied to the oil composition data to determine the composition of each sub-fraction given in Figure 3:

- We assume that saturates can be distinguished from aromatics below the C_{10} carbon cut.
- Since 72.3% mass of the stock tank oil are made up of saturate components (from SARA fractionation analysis of the example oil in this work), 72.3% mass of the materials from the higher carbon cuts (the C_{10} cut and higher) are assumed to be saturate components. The remaining 27.7% (mass) of the materials are assumed to be either aromatics+resins (up to, and including the C_{29} cut) or aromatics+resins and asphaltenes (in the C_{30+} cut).
- The asphaltene fraction accounts for 2.5% mass (from SARA analysis) of the stock-tank oil, and all asphaltenes are found in the C_{30+} sub-fraction.
- The molecular weight distribution (and thus the average molecular weight) of the C_{30+} saturates follows an exponential distribution in mole amount
- The components in the saturates sub-fraction are all normal alkanes.

Based on these assumptions, the average molecular weights were first determined and the PC-SAFT parameters subsequently obtained (from correlations in terms of average molecular weight in Figure 2) for the saturates pseudo-components. The parameters are presented in Table 2. Binary interaction parameters are presented in Table 3 based on fits of vapor-liquid equilibria

data for saturates. SAFT is one of the few equations of state capable of accurately predicting liquid-liquid equilibria based on binary interaction parameters fit to vapor-liquid equilibria data.

In the case of the aromatics+resins pseudo-component, the PC-SAFT parameters depend not only on the average molecular weight but also on the average aromaticity of the sub-fraction. This is because the aromatics+resins sub-fraction is a mixture of aromatics, polynuclear aromatics (PNA), PNA derivatives, and resins. Since the PC-SAFT parameters for compounds in each of these classes follow different parameter correlation curves, it is important to quantify this "degree of aromaticity". An aromaticity parameter was defined to interpolate between parameters for PNA's and those for aromatic derivatives. For a stock tank oil, the degree of aromaticity was adjusted (1) to match the stock tank oil density and (2) so that a "model" n-C_7 insoluble asphaltene is completely soluble in a fluid composed of only the aromatics+resins fraction. Hence, the aromatics+resins pseduo-component possesses the minimum degree of aromaticity necessary to dissolve asphaltenes. The binary interaction parameter between the saturates and the aromatics+resins pseudo-components are set to –0.01 based on the optimal kij for toluene-dodecane and toluene-hexadecane VLE data[57] at 353K and 333K.

At this point, all PC-SAFT parameters have been determined except for the parameters for the asphaltenes. We fit the PC-SAFT parameters for asphaltenes to data for asphaltene precipitation on n-alkane titration of the stock tank oil (see Figure 4). For the oil illustrated in this work, the refractive index of the mixture at the initial point of asphaltene precipitation (P_{RI}) was measured by Wang and Buckley.[58] The P_{RI} is related to the composition and density of the oil; it can also be correlated to the solubility parameter of the oil. In measuring the P_{RI}, the stock-tank oil was

initially mixed with an equal volume of alpha-methyl naphthalene to re-dissolve any precipitated material. For a given oil/precipitant pair, the addition of asphaltene solvents to the oil shifts the amount of precipitant needed to induce asphaltene precipitation but does not significantly alter the refractive index at precipitation onset.[59] By simulating these experiments using PC-SAFT, we are able to fit the three PC-SAFT parameters for asphaltenes to reproduce the P_{RI} behavior. In these calculations, to minimize the number of adjustable parameters, the binary interaction parameters between asphaltenes and the other stock-tank oil components (and alpha-methyl-naphthalene) were set to zero. Using these asphaltene parameters PC-SAFT predicts a solubility parameter for the asphaltene of 21.85 $MPa^{0.5}$ that is consistent with values reported in the literature.[5, 15, 22]

II.C Comparison of Results & Analysis of Asphaltene Behavior

The fit of asphaltene parameters to titration data is shown in Figure 4 in terms of the refractive index of the mixture at the initial point of asphaltene precipitation (P_{RI}). Although the asphaltene parameters were fit to ambient condition alkane titration experiments (for an oil blended with an equal volume of alpha-methyl naphthalene), our experience is that these same asphaltene parameters are applicable for asphaltenes in uncontaminated oil at reservoir conditions. PC-SAFT parameters for the asphaltene component are given in Table 2. This asphaltene has a PC-SAFT calculated solubility parameter of 21.85 $MPa^{0.5}$ and a molar volume of 1,437 cm^3/mol. Given that the density of asphaltenes is estimated to be between 1.13 g/cm^3 and 1.20 g/cm^3, the SAFT calculated stock-tank oil asphaltene has an implied *MW* between 1,624 and 1,724. Because the asphaltenes are assumed to be pre-aggregated in the oil, this reflects the *MW* for the pre-aggregated asphaltenes.

A comparison of PC-SAFT-predicted and experimental densities for the one-phase recombined oil with a gas-oil ratio of 152 m^3/m^3 (for the reservoir fluid) and a GOR of 212 m^3/m^3 (for the reservoir fluid with additional separator gas added) is shown in Figure 5. Although PC-SAFT slightly under-predicts the recombined oil densities, the predicted densities are in good agreement with experimental values.

The PC-SAFT predicted asphaltene instability onset and bubble point pressures for the example recombined oil at reservoir temperature (71.1°C) are plotted versus experimental results in Figure 6 as a function of separator gas composition (corresponding to GORs' of 152 m^3/m^3 and 212 m^3/m^3). PC-SAFT accurately predicts both the bubble points and the asphaltene instability onset points for this oil in the composition range investigated. According to the equation of state calculations, we would expect asphaltene precipitation problems to occur at higher pressure for higher separator gas concentrations.

Consider what is predicted to happen on reservoir depressurization in Figure 6. If we imagine a reservoir fluid at 0.2 mass fraction of gas and 10,000 psia, the asphaltenes are soluble in the oil. On reservoir depressurization to just below 8,000 psia, asphaltenes begin to come out of solution. On further depressurization, we reach the bubble point of the oil where the light ends begin to come out of solution. As the pressure is decreased further, more light ends leave the solution until at just below 3,000 psia, the oil becomes stable for asphaltenes again. This explains the field observation that asphaltenes precipitate only in a certain pressure range. Of course, the

effect of asphaltene re-dissolution kinetics, which may be significant, is not considered in the thermodynamic model.

We find similar phase behavior on N_2 injection for an oil studied by Jamaluddin , et al.[60] In this system, the parameters for the components in the oil are determined by the same approach as previously explained in this chapter. One difference is that N_2 and CO_2 are treated as separate components because each is present in reasonably high concentration. Also, the parameters for the asphaltene component are fit to the asphaltene instability pressure prior to N_2 injection. Details of the calculations are presented in reference (61). A comparison of PC-SAFT results with experimental results is given in Figure 7. The injection of 5, 10, and 20 mole% of N_2 strongly increases the asphaltene instability onset. The oil is originally unstable probably due to its initial high content of CO_2 . The difference between the asphaltene onset pressure and the bubble point pressure ($P_{onset} - P_{bbp}$) increases with the amount of injected N_2. The SAFT predictions closely follow the experimental findings.

For this same system before N_2 injection, the pressure / temperature isopleth projection of the phase diagram has been measured. In Figure 8 we compare the asphaltene onset as a function of temperature with experimental data.[60] PC-SAFT predicts, in qualitative agreement with experiment, asphaltene instability at low temperature and at high temperature. This type of phase boundary is commonly seen in mixtures of components with large size asymmetry. At low temperature, differences in van der Waals interactions and molecular size between the asphaltene molecules and solvent (crude oil) cause phase separation. At high temperature, the oil becomes a

poor solvent and the solution demixes because the light components cause the oil to expand with increase in temperature.

II.D Effect of Asphaltene Polydispersity on Phase Behavior

Results thus far have shown[19, 20, 61] that PC-SAFT can adequately describe asphaltene phase behavior in a recombined oil under reservoir conditions. In these calculations the asphaltenes were treated as a single, monodisperse component in oil. Since asphaltenes are, in actuality, a polydisperse class of compounds with resins as their lowest molecular weight sub-fraction, the effects of asphaltene polydispersity need to be considered.

Here we examine the effect of asphaltene polydispersity on asphaltene's thermodynamic phase behavior in oil. We will show that the lowest molecular weight asphaltenes (including the resins) can stabilize, via nonpolar interactions, the higher molecular weight asphaltenes. We also show, via modeling analyses, qualitative differences in the behavior of the various asphaltene (and resin) sub-fractions. The polydispersity of asphaltenes has been observed in the laboratory, both in terms of the amount of asphaltenes precipitated with various alkane precipitants and in the characterization of the precipitated asphaltenes as "hard" or "soft" asphaltenes. Since deposition tendencies onto pipeline surfaces have often been associated with variations in the morphology and the composition of the precipitated asphaltene phase, an understanding of the molecular weight distribution of polydisperse asphaltenes in equilibrium phases should help us gain a better understanding of the various asphaltene sub-fraction's deposition tendencies.

In this section of the work, polydisperse asphaltenes are represented as four pseudo-components in SAFT. These pseudo-components are denoted n-C_{i-j}, representing the asphaltene fraction insoluble in the n-alkane of carbon number n-C_i, but soluble in the n-alkane n-C_j. Thus, the pseudo-components are denoted n-C_{3-5}, n-C_{5-7}, n-C_{7-15}, and n-C_{15+}. Hence, n-C_{15+} asphaltenes are the asphaltenes fraction insoluble in pentadecane. This assumes, for example, that no n-C_{7-15} asphaltene will precipitate on addition of pentadecane. We will see that there is some co-precipitation, leading to an iterative division of pseudo-components. Since we are interested in the qualitative effects of polydispersity at this point, we consider these pseudo-components suitable for our purposes. The reader should keep in mind that, traditionally, the n-C_{3-5} fraction is called resins and that conventional asphaltene extraction techniques generally identify asphaltenes as the n-C_{5+} or n-C_{7+} insoluble fractions of heavy organics. All asphaltene sub-fractions in this work are soluble in aromatic solvents (assessed via the PC-SAFT equation of state).

II.D.1 Selection of PC-SAFT Parameters for Polydisperse Asphaltenes

In experiments performed by Wang,[14] the asphaltenes from an oil were separated into various solubility fractions using excess n-pentane, n-heptane, and n-pentadecane precipitants; these sub-fractions are called n-C_5 insoluble asphaltenes, n-C_7 insoluble asphaltenes, and n-C_{15} insoluble asphaltenes, respectively. The asphaltene instability onsets with n-alkane titrations were measured for mixtures of toluene with each isolated asphaltene sub-fraction (at ambient conditions and with an asphaltene/toluene ratio of 1 g per 100mL toluene). The experimental asphaltene fractionation and titration data for Lagrave oil from Wang[14] were used to fit parameters for each asphaltene pseudocomponent.

Using this model, we could then study how polydispersity and resins affect the stability of asphaltenes. Although each sub-fraction, including the resins, is polydisperse, we model asphaltenes as either 3 or 4 pseudo-components (depending on whether the resin fraction, which is the n-C_{3-5} asphaltene sub-fraction, was included): an n-C_{15+} sub-fraction, an n-C_{7-15} sub-fraction, an n-C_{5-7} sub-fraction, and an n-C_{3-5} sub-fraction. The method used to fit the SAFT parameters for each asphaltene pseudo-component was similar in principle to the monodisperse SAFT asphaltene characterization procedure discussed above and given in Ting, et al.[19, 20]. Succinctly:

(1) SAFT parameters were fit for the n-C_{15+} asphaltene sub-fraction to reproduce the experimental data on the minimum volume fraction of alkane precipitant needed to induce asphaltene instability (ϕ_v^{ppt}) for mixtures of n-C_{15} insoluble asphaltene, toluene, and various n-alkanes (see Figure 9).

(2) The asphaltene made from the combination of n-C_{15+} and n-C_{7-15} sub-fractions were assumed to represent the n-C_7 insoluble asphaltenes; a second set of SAFT parameters were fit for the n-C_{7-15} sub-fraction to reproduce (together with the previously fitted n-C_{15+} sub-fraction) the experimental ϕ_v^{ppt} data for a mixture of n-C_7 insoluble asphaltene, toluene, and n-alkane as shown in Figure 9.

(3) A third set of SAFT parameters were fit for the n-C_{5-7} sub-fraction so that the combination of the n-C_{15+} (fitted in Step (1)), n-C_{7-15} (fitted in Step (2)), and n-C_{5-7}

sub-fractions represented the n-C_5 insoluble asphaltenes and reproduced the experimental ϕ_v^{ppt} data for a mixture of n-C_5 insoluble asphaltene, toluene, and n-alkanes as shown in Figure 9.

(4) Due to lack of precipitation data, the PC-SAFT parameters for the resin (n-C_{3-5}) sub-fraction were obtained by decreasing the PC-SAFT parameters (m and ε/k) of the n-C_{5-7} asphaltene sub-fraction until a set of PC-SAFT parameter was obtained that would make the resins insoluble in propane (tested at 10 bars) and soluble in n-pentane.

Because there is insufficient data to uniquely fit all of the model parameters for polydisperse asphaltenes, certain approximations and relationships have to be made:

- The molecular weights of all PC-SAFT asphaltene sub-fractions were set to be linearly dependent on chain length, m. This was done because the experimental molecular weight of each asphaltene sub-fraction is not known and because the SAFT chain length is roughly linearly dependent on molecular weight for polynuclear aromatics. The constant of proportionality (MW=m/0.0216) used in this work was set to give the n-C_{15+} asphaltene sub-fraction a molecular weight of 2,500.

- The segment diameters of all asphaltene sub-fractions were set to 4 Angstroms. This is an average value of the segment diameters for most polynuclear aromatics and polynuclear aromatics derivatives.

A comparison of the equation-of-state fitted and the experimental ϕ_v^{ppt} data is shown in Figure 9, with the fitted PC-SAFT asphaltene parameters listed in Table 4. As seen in the figure, the agreement between PC-SAFT calculated and measured ϕ_v^{ppt} is qualitative. PC-SAFT is able to describe the change in magnitude (and to a lesser extent, the curvature) of the ϕ_v^{ppt} vs. n-alkane carbon number curve between n-C_{15} insoluble and n-C_5 insoluble asphaltenes. For the precipitation onsets with n-C_7 and n-C_5 extracted asphaltenes, PC-SAFT underestimates the experimental ϕ_v^{ppt} data in cases where larger n-alkanes (undecane and higher) are used to induce asphaltene precipitation. As seen in the figure, PC-SAFT predicts a maximum in the volume fraction of precipitant at a carbon number of about 9, in agreement with previous experimental observations.

A plot of the SAFT parameters ε/k vs. m for the various SAFT asphaltene sub-fractions and resin (the n-C_{3-5} sub-fraction) shows a well-defined trend between ε/k and m (Figure 10). The asphaltenes precipitated by the lower molecular weight n-alkanes tend to be smaller in size and have lower segment energy. It is also interesting to note that despite having the same segment size, the segment energy of the "heavier" asphaltene sub-fractions seem to be larger. The asphaltene sub-fractions have a segment energy close to that for naphthalene and alpha-methylnaphthalene (Table 1 and Figure 2); however, the chain lengths, m, of the asphaltenes are much larger. Finally, the chain length (m) for the resin sub-fraction seems to be much smaller than the other asphaltene sub-fractions. Equation of state parameters for the asphaltene and resin fractions are given in Table 4.

II.D.2 Effects of Asphaltene Polydispersity and Resin Addition

To investigate the roles resins and asphaltene polydispersity play on asphaltene phase behavior in oil, we will compare the phase behavior of four model oil mixtures containin monodisperse or polydisperse asphaltenes. In all model systems, toluene is the model oil and the asphaltenes have a fixed concentration of 7.5 g asphaltenes to 100 mL of toluene. The properties and asphaltene/resin contents of these systems are listed in Table 5 and are discussed in the following paragraph. For these model system investigations, the focus is on the qualitative trends/behaviors and all binary interaction parameters between all species are set to zero (following Ting, *et al.* [19, 20]).

The biggest difference between the various systems in Table 5 is that asphaltenes in Systems 1 and 2 are monodisperse, while the asphaltenes in Systems 3 and 4 are polydisperse. More specifically, the asphaltene used in Model System 1 is monodisperse and was fit to experimental ϕ_v^{ppt} data for the n-C_{15} insoluble Lagrave asphaltenes[14] (also called the n-C_{15+} asphaltene fraction in this work). The asphaltene used in Model System 2 is monodisperse and was fit to experimental ϕ_v^{ppt} data for the n-C_5 insoluble Lagrave asphaltenes. The asphaltene used in Model System 3 is polydisperse and the SAFT parameters for each asphaltene sub-fraction were fit to the experimental ϕ_v^{ppt} data of the fractionated asphaltenes. Model System 4 is similar to Model System 3 with the exception that 10g of resin per 100mL toluene (approximately 1-2 moles resin/100moles toluene) is added to the system. The amount of resin added (10g resin per 100mL toluene) is arbitrary.

The effects of n-alkane addition on the amount of asphaltenes precipitated (at 20°C and 1 bar) for the four model oil mixtures are shown in Figures 11 and 12. For systems containing monodisperse asphaltenes (Figure 11), the change in asphaltene solubility is dramatic: asphaltenes go from completely soluble to almost completely insoluble in the model oil when the volume fraction of the n-alkane precipitant is increased slightly past the asphaltene instability onset point. As expected, the lower molecular weight asphaltenes (the monodisperse asphaltene fit to the n-C_5 insoluble asphaltenes ϕ_v^{ppt} data) are more soluble than the higher molecular weight asphaltene (the monodisperse, n-C_{15} insoluble asphaltene) in terms of the amount of precipitant needed to induce asphaltene instability. When sufficiently large amount of n-alkanes are added to the model oil, all asphaltenes will precipitate.

A large change in the amount of precipitated asphaltenes vs. precipitant volume fraction can be seen when the effect of asphaltene polydispersity (and resin addition) is taken into consideration (Figure 12). By treating asphaltene as a polydisperse specie, the amount of asphaltenes precipitated increases much more gradually with precipitant addition. A significant amount of asphaltenes will stay in solution even at high precipitant volume fractions, and more asphaltenes can be precipitated using lower molecular weight n-alkanes. It is interesting to note that when n-C_{15} is used as the precipitant, SAFT predicts the existence of a solubility minimum around ϕ_v^{ppt}=0.9.

A comparison of the SAFT-predicted behavior of polydisperse asphaltenes with and without resins show that the presence of resins will increase the amount of precipitant needed to induce the onset of asphaltene instability (Figure 12). Furthermore, at lower precipitant volume

fractions in the oil, the amount of asphaltenes that will precipitate is less when resins are present. Even though only dispersion interactions are considered in these PC-SAFT models, the lower molecular weight asphaltenes and especially resins will stabilize the heavier asphaltenes in the oil. It can be seen in Figure 12 that the effects of resins on asphaltene phase behavior in the oil become less pronounced as the oil is diluted more with precipitants.

A plot of the mass distribution of the asphaltene sub-fractions as a function of precipitant volume fraction is shown in Figure 13. As seen in the figure, near the initial asphaltene instability onset, the precipitated phase is composed mostly of the heaviest asphaltene fractions (in this case, the n-C_{15+} sub-fraction). As the amount of precipitant is increased further, more and more lower molecular weight asphaltenes will precipitate.

III. Summary & Conclusions

The effect of pressure, temperature, and composition on the phase behavior of asphaltenes in crude oil systems can be explained in terms of van der Waals interactions between molecules using the PC-SAFT equation of state. A method was introduced to characterize the recombined oil including asphaltenes as a six-component mixture using the PC-SAFT equation of state. The real components and pseudo-components were chosen based on saturates-aromatics-resins-asphaltenes (SARA) fractionation, gas chromatography, and gas-oil ratio information. Equation of state parameters for each component (except asphaltenes) were determined from generalized correlations in terms of molecular weight. Binary interaction parameters were fit to vapor liquid equilibria data. Asphaltene parameters were determined by modeling asphaltene precipitation upon titration of oil with n-alkanes at ambient conditions. PC-SAFT was found to accurately

predict the density, the bubble point curve and the asphaltene instability region for the recombined oil over a range of temperatures, pressures, and compositions.

The PC-SAFT equation of state has proved useful in explaining laboratory and field observations of asphaltene phase behavior. For example, when asphaltene precipitates near the bubble point, the model predicts asphaltene stability at high pressure and at pressures well below the bubble point. On titration of the oil with various n-alkanes, we show that the volume fraction of precipitant required for asphaltene precipitation as a function of carbon number of the alkane precipitant reaches a maximum at about nonane. The model also predicts that asphaltenes can become unstable as temperature is decreased or increased depending on the composition of the oil and the temperature. The model has also proved to be predictive in describing the effect of gas injection (nitrogen and methane) and of alpha methyl naphthalene on asphaltene stability.

We have investigated the effect of polydispersity and resins on asphaltene phase behavior for a model system. We find that resins delay the onset of asphaltene precipitation, but the total amount of asphaltene precipitated is unaffected by the resins. SAFT calculations show that the lower molecular weight asphaltenes and resins play a large role in stabilizing higher molecular weight asphaltenes in oil. Resin's stabilizing effects on polydisperse asphaltene is greatest in the region of incipient asphaltene instability; when sufficiently large amounts of n-alkane precipitants are added, similar amounts of asphaltenes would precipitate regardless of the presence of resins in the oil. An analysis of the mass distribution of the asphaltene sub-fractions in the precipitated phase shows that the largest asphaltenes will precipitate first, followed by the

precipitation of smaller asphaltenes upon further oil dilution. In our study, the heaviest asphaltene sub-fraction precipitated first.

The amount and type of data presently available for onset of asphaltene precipitation can be adequately modeled without including the effect of polar groups or association. Although extensions of the PC-SAFT equation of state can account for these effects, presently available data is insufficient to justify the additional parameters needed to include these effects.

Acknowledgements

We gratefully acknowledge the Department of Energy, DeepStar, ChevronTexaco, DB Robinson, and the Consortium of Processes in Porous Media at Rice University for their financial support. We also thank Jeff Creek and Jill Buckley for many helpful discussions.

References

1 W.G. Chapman, G. Jackson, and K.E. Gubbins, *Mol. Phys.* **65,** 1057-1079, (1988).
2 W.G. Chapman, K.E. Gubbins, G. Jackson, and M. Radosz, *Fluid Phase Equil.* **52,** 31-38, (1989).
3 W.G. Chapman, K.E. Gubbins, G. Jackson, and M. Radosz, *Ind. Eng. Chem. Res.* **29,** 1709-1721, (1990).
4 J. Gross,. and G. Sadowski, *Ind. Eng. Chem. Res.* **40,** 1244-1260, (2001).
5 I.A. Wiehe and K.S. Liang, *Fluid Phase Equil.* **117,** 201-221, (1996).
6 C.E. Haskett and M. Tartera, *J. Pet. Tech.* **17,** 387-391, (1965).
7 R.N. Tuttle, *J. Pet. Tech.* **35,** 1192-1196, (1983).
8 S. Adialalis, *Investigation of physical and chemical criteria as related to the prevention of asphalt deposition in oil well tubings.* Ph.D. Thesis, Imperial College, 1982
9 A.J.L. Chavez and M.A. Lory, *Revista del Instituto Mexicano del Petroleo* **23,** 1, (1991).
10 J. Escobedo and G.A. Mansoori, in *SPE Annual Technical Conference and Exhibition* (Dallas, TX, 1995).
11 C. von Albrecht, W.M. Salathiel, and D.E. Nierode, *CIM Special Volume* **,** 55-62, (1977).

12 J. Wu, *Molecular Thermodynamics of Some Highly Asymmetric Liquid Mixtures,* Ph.D. Thesis, University of California at Berkeley, 1998.
13 J.M. Prausnitz, R.N. Lichtenthaler, and E.G. de Azevedo, *Molecular Thermodynamics of Fluid-Phase Equilibria*, 2nd ed. P T R Prentice-Hall, Inc., 1986.
14 J.X. Wang, *Predicting Asphaltene Flocculation in Crude Oils,* Ph.D. Thesis, New Mexico Institute of Mining & Technology, 2000.
15 A. Hirschberg, L.N.J. deJong, B.A. Schipper, and J.G. Meijer, J. G., *Soc. Pet. Eng. J.* **24,** 283-293, (1984).
16 K. Akbarzadeh, S. Ayatollahi, M. Moshfeghian, H. Alboudwarej., W.Y. Svrcek, and H.W. Yarranton, in *Amer. Inst. Chem. Eng. Spring National Meeting* (New Orleans, LA, 2002), pp. 218-224.
17 R. Cimino, S. Correra, and P.A. Sacomani, in *Soc. Pet. Eng. Intl. Symp. on Oilfield Chem.* (San Antonio, TX, 1995).
18 L.X. Nghiem, M.S. Hassam, R. Nutakki, and A.E.D. George, in *Soc. Pet. Eng. Annual Tech. Conf. and Exhib.* (Houston, TX, 1993), pp. 375-384.
19 P.D. Ting, G.J Hirasaki, and W.G. Chapman, *Pet. Sci. Tech.* **21**, 647-661, (2003).
20 P.D. Ting, *Thermodynamic Stability and Phase Behavior of Asphaltenes in Oil and of other highly Asymmetric Mixtures,* Ph.D. Thesis, Rice University, 2003.
21 F. Chung, P. Sarathi, and R. Jones, (National Institute for Petroleum and Energy Research, Bartlesville, 1991).
22 N.E. Burke, R.E. Hobbs, and S.F. Kashou, *J. Pet. Tech.* **42,** 1440-1446 (1990).
23 J.X. Wang, J.S. Buckley, N.A. Burke, and J.L. Creek, paper 15254 presented at the 2003 SPE Offshore Technology Conference, Houston, May 5-7; J.X. Wang and J.S. Buckley, *Energy & Fuels*, **15**, 1004-1012, (2001).
24 L.X. Nghiem and D.A. Coombe, *Soc. Pet. Eng. J.* **2** (1997).
25 P.D. Ting, P.C. Joyce, P.K. Jog, W.G. Chapman, and M.C. Thies, *Fluid Phase Equil.,* (2002).
26 K.J. Leontaritis. and G.A. Mansoori, in *Soc. Pet. Eng. Intl. Symp. on Oilfield Chem.* (San Antonio, TX, 1987).
27 A.I. Victorov and A. Firoozabadi, *Amer. Inst. Chem. Eng. J.* **42,** 1753-1764, (1996).
28 J. Wu, J.M. Prausnitz, and A. Firoozabadi, *Amer. Inst. Chem. Eng. J.* **44,** 1188-1199, (1998).
29 J. Wu, J.M. Prausnitz, and A. Firoozabadi, *Amer. Inst. Chem. Eng. J.* **46,** 197-209, (2000).
30 Bungert, B. Komplexe Phasengleichgewichte von Polymerlösungen. *Dissertation*, Technische Universität Berlin, Germany, *1998*; J. Gross and G. Sadowski, *Ind. Eng. Chem. Res.*, **41**, 1084-1093, (2002).
31 I.A. Wiehe, *Fuel Sci. Tech. Intl.* **14,** 289-312, (1996).
32 E.W. Moore, C.W. Crowe, and A.R. Hendrickson, *J. Pet. Tech.* **17,** 1023-1028, (1965).
33 C.L. Chang and H.S. Fogler, in *Soc. Pet. Eng. Intl. Symp. on Oilfield Chem.* (New Orleans, LA, 1993).
34 H. Groenzin and O.C. Mullins, *J. Phys. Chem. A,* **103,** 11237-11245, (1999).
35 I.G. Economou, *Ind. Eng. Chem. Res.* **41,** 953-962, (2002).
36 E.A. Muller. and K.E. Gubbins, *Ind. Eng. Chem. Res.* **40,** 2193-2212, (2001).
37 P.K. Jog, W.G. Chapman, S.K. Gupta, and R.D. Swindoll, *Ind. Eng. Chem. Res.*, **41**, 887-891, (2002).

38 M.S. Wertheim, *J. Stat. Phys.* **35,** 19, (1984).
39 M.S. Wertheim, *J. Stat. Phys.* **35,** 35, (1984).
40 M.S. Wertheim, *J. Stat. Phys.* **42,** 459, (1986).
41 M.S. Wertheim, *J. Stat. Phys.* **42,** 477, (1986).
42 W.G. Chapman, *J. Chem. Phys.*, **93**, 4299-4304, (1990).
43 T. Kraska and K.E. Gubbins, *Ind. Eng. Chem. Res.*, **35**, 4727-4737, (1996); *Ind. Eng. Chem. Res.*, **35**, 4738-4746, (1996)
44 A. GilVillegas, A. Galindo, P.J. Whitehead, S.J. Mills, G. Jackson, A.N. Burgess, *J. Chem. Phys.*, **106**, 4168-4186 (1997).
45 S.H. Huang and M. Radosz, *Ind. Eng. Chem. Res.* **29,** 2284-2294, (1990).
46 DIPPR, (AIChE, 2003).
47 P.D. Ting, J. Wang, J.S. Buckley, J. Creek, A. Hamammi, G.J. Hirasaki, and W.G. Chapman, *In Preparation*, (2005).
48 A.F. Kidnay, R.C. Miller, W.R. Parrish, and M.J. Hiza, *Cryogenics* **15,** 531-540, (1975).
49 H.H, Reamer, B.H. Sage, and W.N. Lacey, *Ind. Eng. Chem.* **42,** 534, (1950).
50 L. Grauso, A. Fredenslund, and J. Mollerup, *Fluid Phase Equil.* **1,** 13-26, (1977).
51 H.H. Reamer, R.H. Olds, B.H. Sage, and W.N. Lacey, *Ind. Eng. Chem.* **34,** 1526-1531, (1942).
52 M. Elbishlawi and J.R. Spencer, *Ind. Eng. Chem.* **43,** 1811-1815, (1951).
53 A. Azarnoosh and J.J. McKetta, *J. Chem. Eng. Data* **8,** 494-496, (1963).
54 P.C. Joyce, *Vapor-Liquid Equilibria for Long-Chain Hydrocarbons in Supercritical Alkane Solvents.* Ph.D. Thesis, Clemson University, 1999; P.C. Joyce, J. Gordon, and M.C. Thies, *J. Chem. Eng. Data* **45,** 424-427, (2000); P.C. Joyce and M.C. Thies, *J. Chem. Eng. Data* **43,** 819-822, (1998).
55 P. Miller and B.F. Dodge, *Ind. Eng. Chem.* **32,** 434-438, (1940).
56 J.W. Glanville, B.H. Sage, and W.N. Lacey, *Ind. Eng. Chem.* **42,** 508, (1950).
57 U. Messow and I. Engel, *Z. Phys. Chem.* **258,** 798, (1977).
58 J.S. Buckley and J. Wang, Private Communication, (2003).
59 J.S. Buckley, G.J. Hirasaki, Y. Liu, S. von Drasek, J. Wang, and B.S. Gill, *Pet. Sci. Tech.* **16,** 251-285, (1998).
60. A.K.M. Jamaluddin, N. Joshi, F. Iwere, and O. Gurnipar, *SPE **74393**,* (2001).
61. D.L. Gonzalez, P.D. Ting, G.J. Hirasaki, and W.G. Chapman, *Energy & Fuels,* **19**, 1230-1234 (2005).

Tables

Table 1. PC-SAFT pure component parameters: m is the number of segments that make up a molecule, σ is the segment diameter in angstroms, ε/k is the interaction energy between a pair of segments in K. For substances fitted by Ting,[20] the AAPDs[a] and temperature range of the experimental data are given.[46] All other PC-SAFT parameters are from Gross and Sadowski.[4]

Substance	MW (g/mol)	m	σ (A)	ε/k (K)	T range (K)	AAPD[a] P^{sat}	AAPD[a] ρ^{liq}
			n-alkanes				
methane	16.04	1.0000	3.7039	150.03			
ethane	30.07	1.6069	3.5206	191.42			
propane	44.09	2.0020	3.6184	208.11			
butane	58.12	2.3316	3.7086	222.88			
pentane	72.15	2.6896	3.7729	231.20			
hexane	86.18	3.0576	3.7983	236.77			
heptane	100.20	3.4831	3.8049	238.40			
octane	114.23	3.8176	3.8373	242.78			
nonane	128.25	4.2079	3.8448	244.51			
decane	142.29	4.6627	3.8384	243.87			
undecane	156.31	4.9082	3.8893	248.82			
dodecane	170.34	5.3060	3.8959	249.21			
tridecane	184.37	5.6877	3.9143	249.78			
tetradecane	198.39	5.9002	3.9396	254.21			
pentadecane	212.42	6.2855	3.9531	254.14			
hexadecane	226.45	6.6485	3.9552	254.70			
eicosane	282.55	7.9849	3.9869	257.75			
			Cycloalkanes				
cyclopentane	70.13	2.3655	3.7114	265.83			
methyl-cyclopentane	84.16	2.6130	3.8253	265.12			
ethyl-cyclopentane	98.18	2.9062	3.8873	270.50			
cyclohexane	84.15	2.5303	3.8499	278.11			
methyl-cyclohexane	98.18	2.6637	3.9993	282.33			
ethyl-cyclohexane	112.22	2.8256	4.1039	294.04			
cyclopheptane	98.19	2.6870	3.9352	296.15	300-570	0.44	0.21
cyclooctane	112.22	2.9222	4.0028	304.67	300-620	0.71	1.06
			polynuclear aromatics				
benzene	78.11	2.4653	3.6478	287.35			
naphthalene	128.17	3.0915	3.8333	348.40	373-633	1.45	0.77
anthracene	178.23	3.5291	4.0922	402.13	500-830	1.81	1.57
phenanthrene	178.23	3.4890	4.1053	403.06	330-780	1.51	1.39
naphthacene	228.29	4.6432	3.8942	407.60	660-940	0.88	4.23
chrysene	228.29	5.1201	3.8400	385.73	580-940	0.81	3.61
pyrene	202.26	3.6847	4.1151	427.35	450-850	1.37	3.76
			aromatic & polynuclear aromatics derivatives				

toluene	92.14	2.8149	3.7169	285.69			
ethylbenzene	106.17	3.0799	3.7974	287.35			
propylbenzene	120.19	3.3438	3.8438	288.13			
butylbenzene	134.22	3.7662	3.8727	283.07			
tetralin	132.21	3.3131	3.8750	325.07			
biphenyl	154.21	3.8877	3.8151	327.42			
1-methylnaphthalene	142.20	3.4064	3.8961	345.71	393-673	0.29	0.50
1-phenylnaphthalene	204.27	4.7634	3.8582	336.53	330-780	1.51	1.39
m-terphenyl	228.29	5.6273	3.7967	329.18	420-840	1.52	0.26
			Gases				
nitrogen	28.01	1.2053	3.3130	90.96			
carbon dioxide	44.01	2.0729	2.7852	169.21			
carbon disulfide	76.14	1.6919	3.6172	334.82			

a Average absolute percent deviation = $\frac{1}{ndp}\sum_{ndp}\left|\frac{Calculated - Experimental}{Experimental}\right|100\%$

Table 2. Fractionation of the recombined oil with GOR = 152 m^3/m^3 into a 6 component mixture.

Component	Mole Fraction	Average MW	*m*	$\sigma(A)$	$\varepsilon/k(K)$
Methane	0.3300	16	1.0000	3.7039	150.03
Nitrogen & Carbon Dioxide	0.0985	28	1.2053	3.3130	90.96
Light Alkanes	0.2234	47	1.9854	3.6917	206.12
Saturates	0.2445	255	7.3765	3.9635	257.12
Aromatics & Resins	0.1023	212	5.3351	3.7637	323.70
Asphaltenes	0.0013	1700*	29.5000	4.3000	395.00

* molecular weight of pre-aggregated asphaltene

Table 3. Binary interaction parameters used in this study.

Component	methane	$N_2 + CO_2$	Light Alkanes	Saturates	Aromatics & Resins	Asphaltenes
methane	0	0[a]	0.01[b]	0.03[d]	0.03[e]	0.03[k]
$N_2 + CO_2$	0[a]	0	0.07[c]	0.01[f]	0.13[h]	0.13[k]
Light Alkanes	0.01[b]	0.07[c]	0	0.006[g]	0.02[i]	0.02[k]
Saturates	0.03[d]	0.01[f]	0.006[g]	0	-0.01[j]	0
Aromatics & Resins	0.03[e]	0.13[h]	0.02[i]	-0.01[j]	0	0
Asphaltenes	0.03[k]	0.13[k]	0	0	0	0

a based on methane-N_2 binary data of Kidnay, *et al.*[48]
b based on methane-propane binary data of Reamer, *et al.*[49]
c based on N_2-propane binary data of Grauso, *et al.*[50]
d based on methane-decane data of Reamer, *et al.*[51]
e based on methane-toluene binary data reported in this work and from Elbishlawi and Spencer[52]
f based on N_2-decane binary data of Azarnoosh and McKetta[53]
g based on propane-hexadecane binary data of Joyce[54]
h based on N_2-benzene binary data of Miller and Dodge[55]
i based on propane-benzene binary data of Glanville, *et al.*[56]
j based on toluene-dodecane and toluene-hexadecane binary data of Messow and Engel[57]
k the *kij*s' between asphaltenes and separator gas sub-fractions are assumed to be the same as the *kij*s' between aromatics+resins and separator gas sub-fractions.

Table 4. PC-SAFT parameters for the various asphaltene sub-fractions (including resins)

		SAFT Parameters				
Asphaltene sub-fraction	MW	*m*	σ (A)	*ε/k* (K)	δ ($MPa^{0.5}$)	ρ (g/cm^3)
n-C_{15+}	2500*	54	4.00	350.5	22.17	1.150
n-C_{7-15}	1852*	40	4.00	340.0	21.52	1.137
n-C_{5-7}	1806*	39	4.00	335.0	21.25	1.133
Resin	556	12	4.00	330.0	20.41	1.103
Monodisperse – n-C_5	2080*	46	4.00	350.5	22.13	1.120

* molecular weight of pre-aggregated asphaltene

Tables 5. Description of four representative model oils tested to study the effects of asphaltene polydispersity and resin addition. All model oils contained 7.5 g of asphaltene to 100 mL of toluene (20°C, 1 bar).

Model System	Included Asphaltene fractions
System 1	Monodisperse – n-C_{15+} subfraction only
System 2	Monodisperse – n-C_5
System 3	n-C_{15+}:n-C_{7-15}: n-C_{5-7} with mass ratios of 4.5 : 2.0 : 3.5
System 4	n-C_{15+}:n-C_{7-15}: n-C_{5-7} with mass ratios of 4.5 : 2.0 : 3.5 and resins 10 g/100 mL toluene (20°C, 1 bar)

Figure Captions

Figure 1. Contributions to the SAFT equation of state for an associating polyatomic fluid.
Figure 2. Plots of PC-SAFT pure component parameters as a function of molecular weight for saturates and polynuclear aromatics.
Figure 3. Representation of a recombined oil with six pseudo-components.
Figure 4. Refractive index at the point of asphaltene precipitation (P_{RI}) from an equi-volume mixture of stock tank oil and alpha-methyl naphthalene on titration with n-alkane. The curve shows results from the PC-SAFT equation of state and the data is from Wang and Buckley.[58]
Figure 5. Experimental[47] and PC-SAFT-predicted (lines) one-phase recombined oil densities with two different gas-oil ratios at 71.1°C.
Figure 6. PC-SAFT-predicted and measured[19, 47] asphaltene instability onset and mixture bubble points for the recombined oil at 71.1°C.
Figure 7. PC-SAFT-predicted and measured[60] asphaltene instability onset and mixture bubble points as a function of nitrogen concentration in a recombined oil at 296°F.
Figure 8. The temperature dependence of the asphaltene instability curve and bubble curve predicted by PC-SAFT and experimental measurements[60] for the reservoir fluid prior to nitrogen injection.
Figure 9. Comparison of PC-SAFT and measured precipitant volume fraction at asphaltene instability onset for asphaltene-toluene-n-alkane mixtures at 20°C and 1 bar. The asphaltene/toluene ratio is 1g/100mL. Experimental data are from Wang[14]
Figure 10. Plot of ε/k vs. m for the various PC-SAFT asphaltene sub-fractions and resin.
Figure 11. Solubility of monodisperse asphaltenes in model oil (7.5g asphaltene/100mL toluene) mixed with n-alkanes at 20°C and 1 bar.
Figure 12. Solubility of polydisperse asphaltenes (with or without resins) in model oil (7.5g total asphaltene/100mL toluene) mixed with n-alkanes at 20°C and 1 bar.
Figure 13. Normalized distribution of the asphaltene sub-fractions in the precipitated phase as a function of volume fraction precipitant in the model oil mixtures.

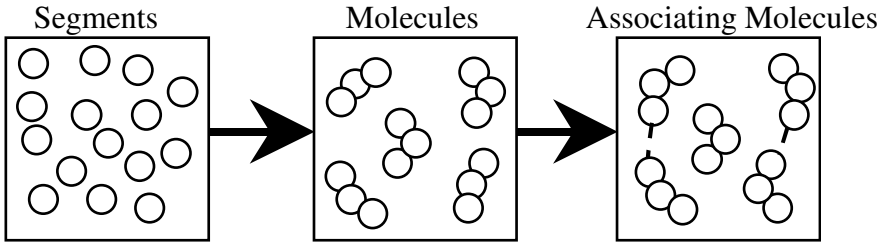

$$A = A^{segment} + \Delta A^{chain} + \Delta A^{assoc}$$

Figure 1. Contributions to the SAFT equation of state for an associating polyatomic fluid.

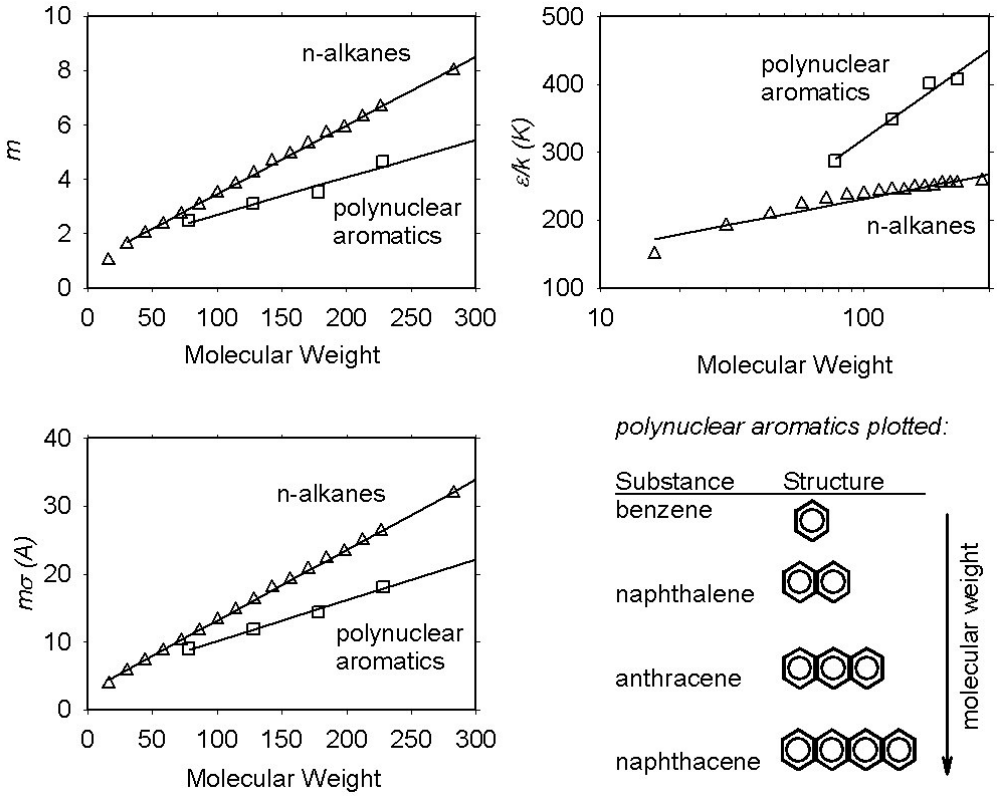

Figure 2. Plots of PC-SAFT pure component parameters as a function of molecular weight for saturates and polynuclear aromatics.

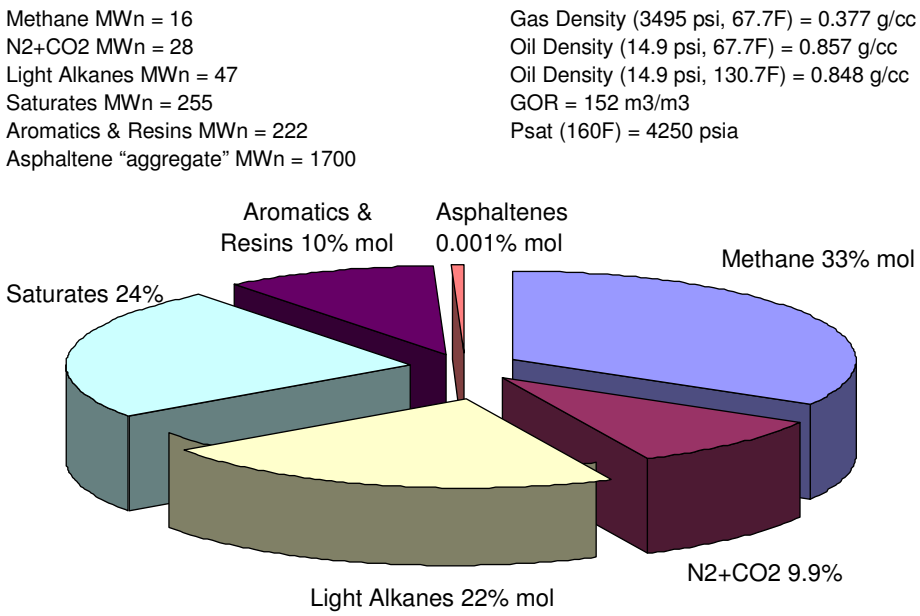

Figure 3. Representation of a recombined oil with six pseudo-components.

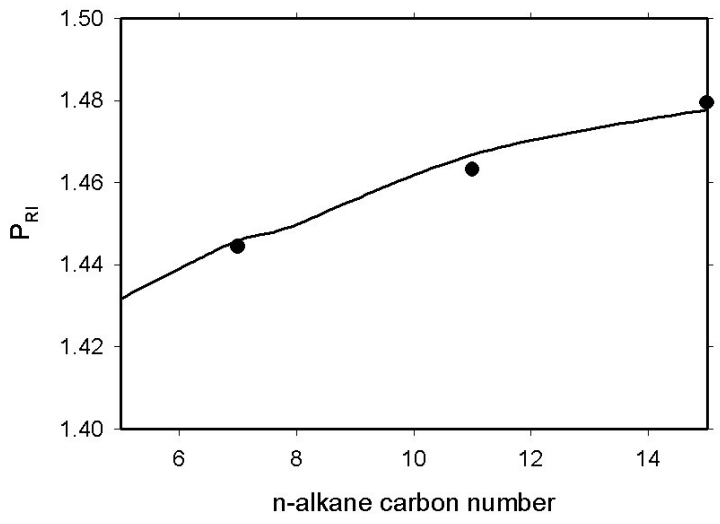

Figure 4. Refractive index at the point of asphaltene precipitation (P_{RI}) from an equi-volume mixture of stock tank oil and alpha-methyl naphthalene on titration with n-alkane. The curve shows results from the PC-SAFT equation of state and the data is from Wang and Buckley.[58]

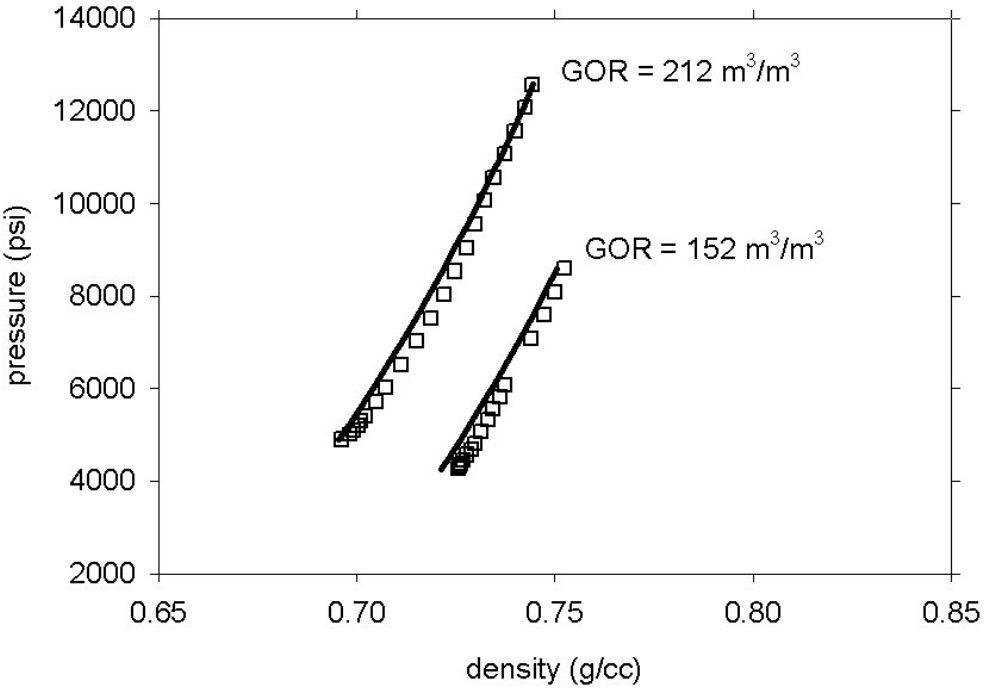

Figure 5. Experimental[47] and PC-SAFT-predicted (lines) one-phase recombined oil densities with two different gas-oil ratios at 71.1°C.

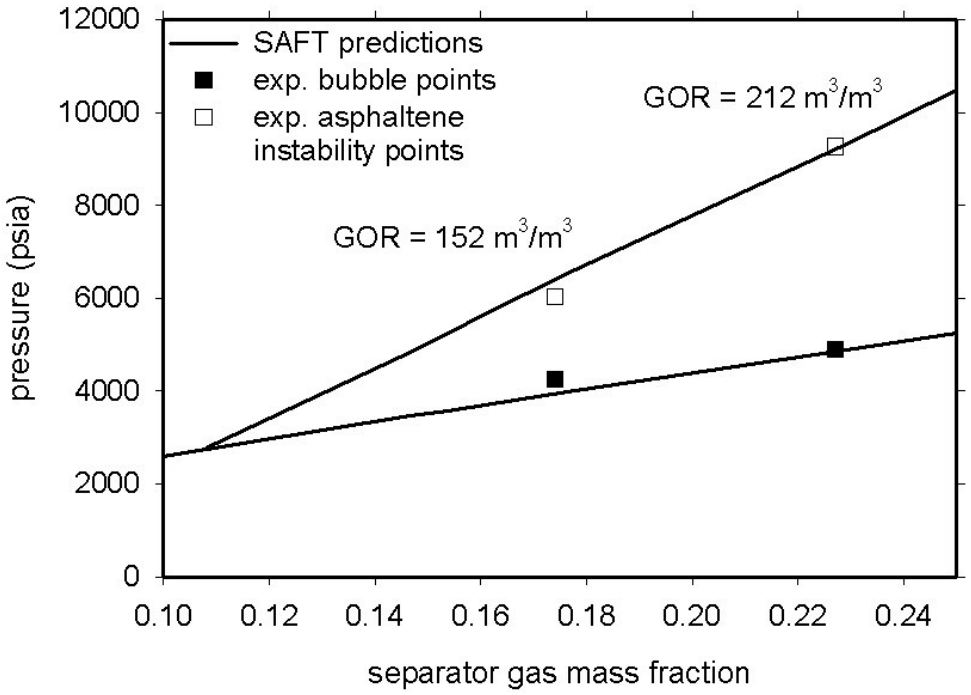

Figure 6. PC-SAFT-predicted and measured[19, 47] asphaltene instability onset and mixture bubble points for the recombined oil at 71.1°C.

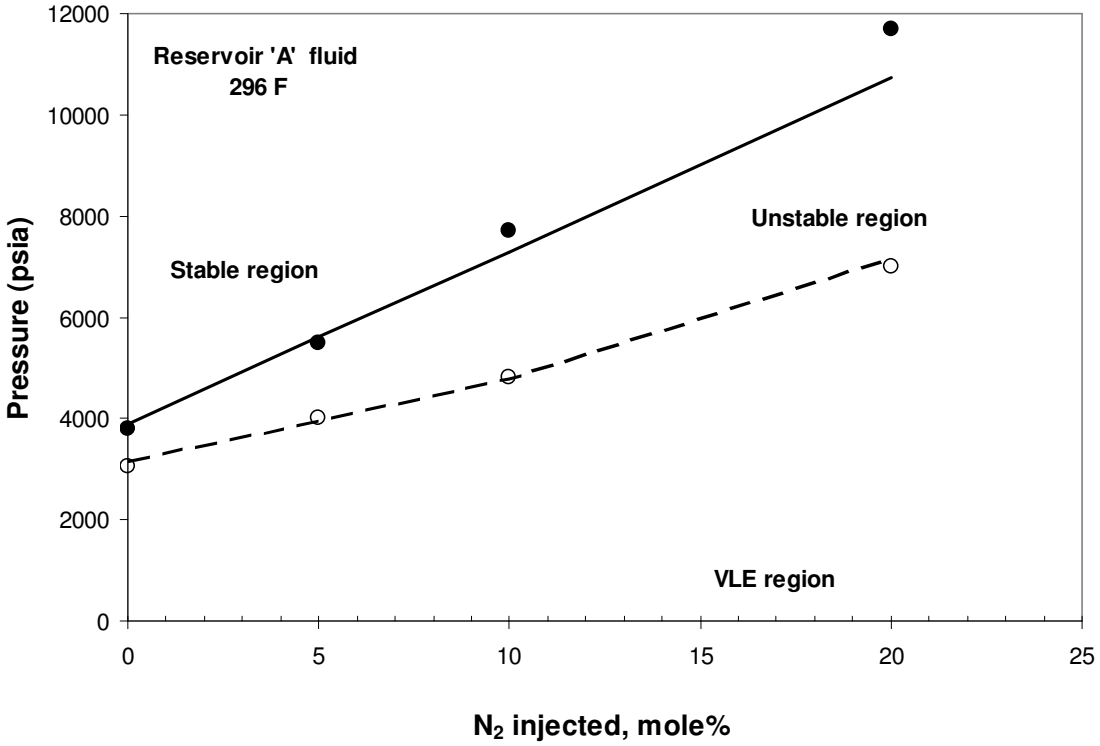

Figure 7. PC-SAFT-predicted and measured[60] asphaltene instability onset and mixture bubble points as a function of nitrogen concentration in a recombined oil at 296°F.

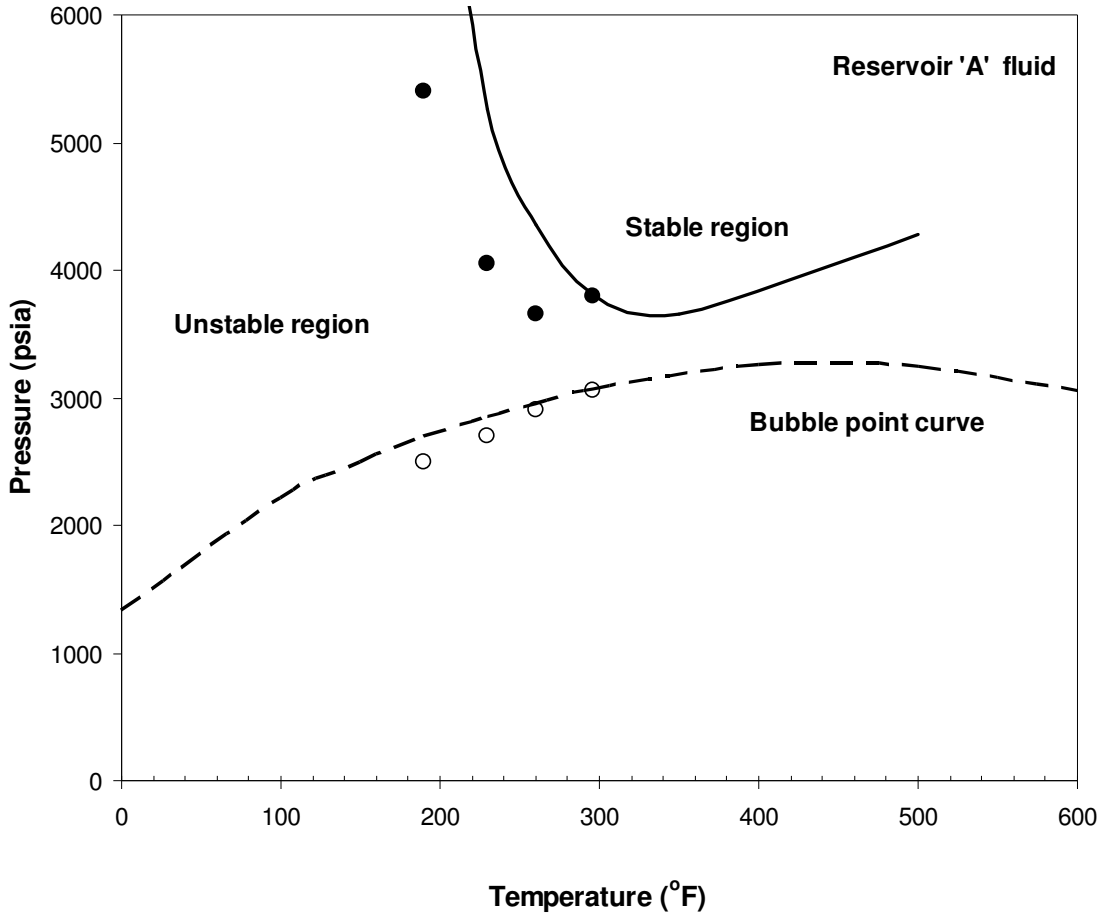

Figure 8. The temperature dependence of the asphaltene instability curve and bubble curve predicted by PC-SAFT and experimental measurements[60] for the reservoir fluid prior to nitrogen injection.

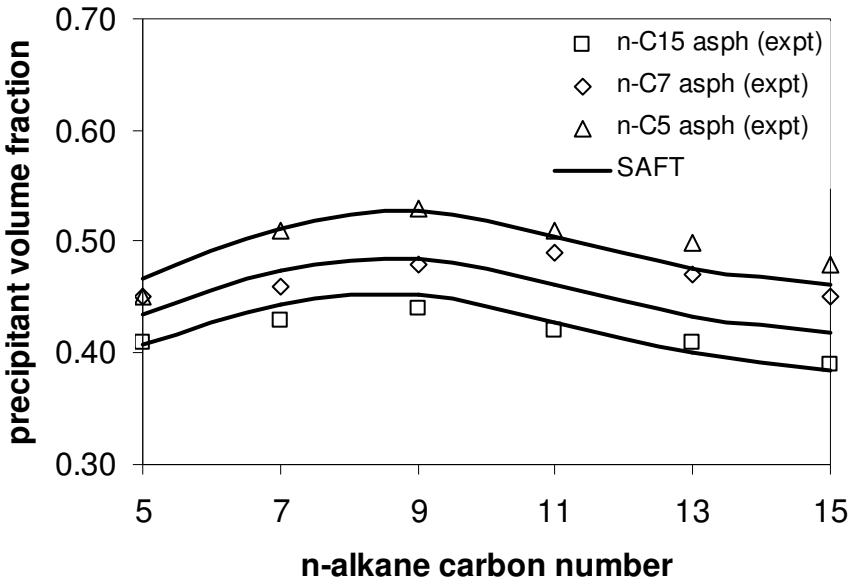

Figure 9. Comparison of PC-SAFT and measured precipitant volume fraction at asphaltene instability onset for asphaltene-toluene-n-alkane mixtures at 20°C and 1 bar. The asphaltene/toluene ratio is 1g/100mL. Experimental data are from Wang[14]

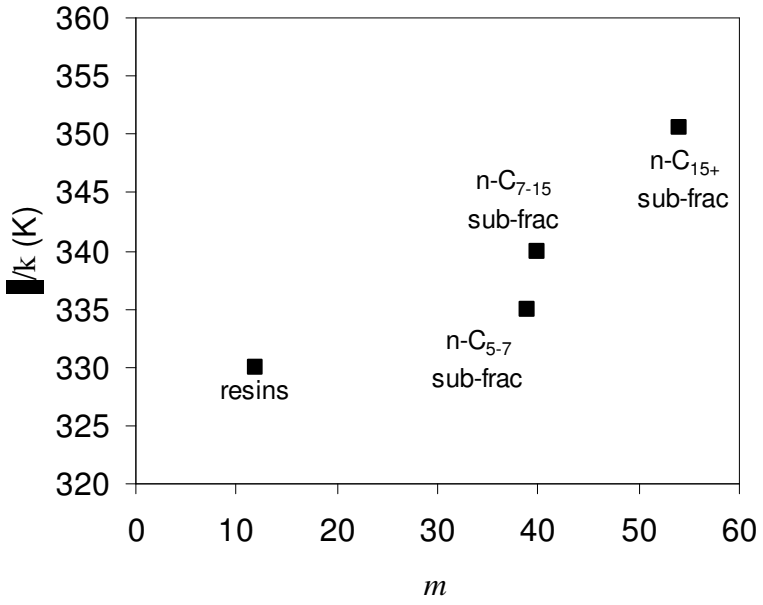

Figure 10. Plot of ε/k vs. m for the various PC-SAFT asphaltene sub-fractions and resin.

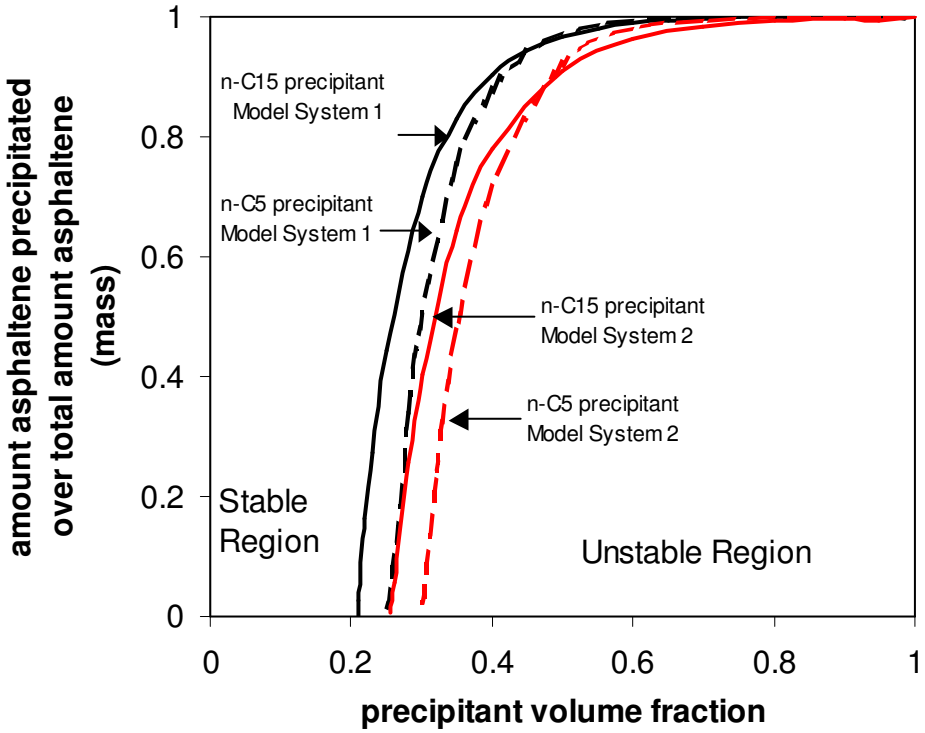

Figure 11. Solubility of monodisperse asphaltenes in model oil (7.5g asphaltene/100mL toluene) mixed with n-alkanes at 20°C and 1 bar.

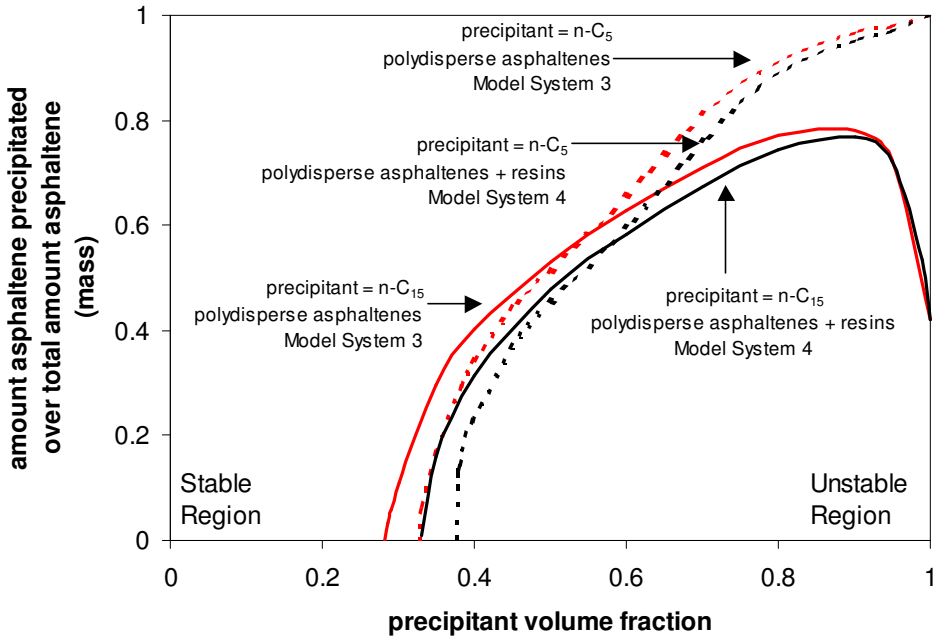

Figure 12. Solubility of polydisperse asphaltenes (with or without resins) in model oil (7.5g total asphaltene/100mL toluene) mixed with n-alkanes at 20°C and 1 bar.

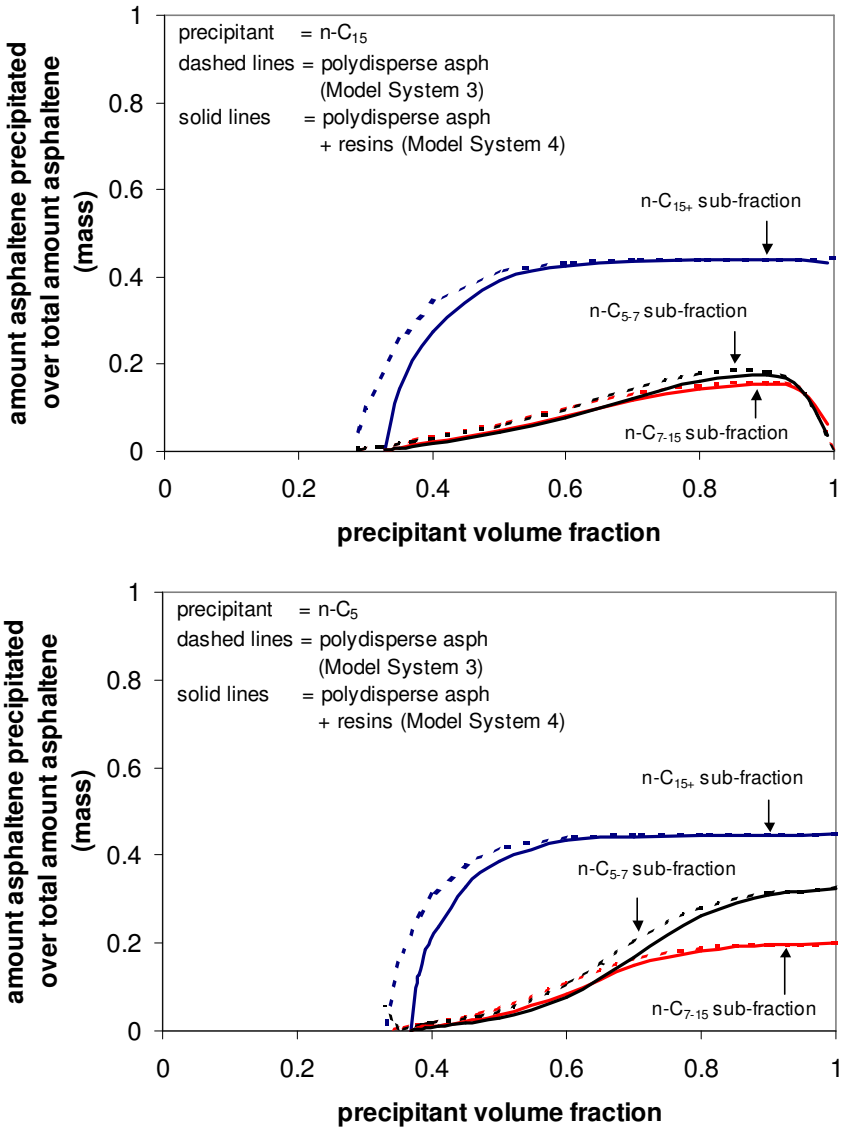

Figure 13. Normalized distribution of the asphaltene sub-fractions in the precipitated phase as a function of volume fraction precipitant in the model oil mixtures.